

# Continuous oxygen ion transfer medium as a catalyst for high selective oxidative dehydrogenation of ethane

Haihui Wang, You Cong and Weishen Yang \*

State Key Laboratory of Catalysis, Dalian Institute of Chemical Physics, Chinese Academy of Sciences, PO Box 110, Dalian 116023, China

Received 26 April 2002; accepted 8 August 2002

An oxygen permeable mixed ion and electron conducting membrane (OPMIECM) was used as an oxygen transfer medium as well as a catalyst for the oxidative dehydrogenation of ethane to produce ethylene.  $O^{2-}$  species transported through the membrane reacted with ethane to produce ethylene before it recombined to gaseous  $O_2$ , so that the deep oxidation of the products was greatly suppressed. As a result, 80% selectivity of ethylene at 84% ethane conversion was achieved, whereas 53.7% ethylene selectivity was obtained using a conventional fixed-bed reactor under the same reaction conditions with the same catalyst at 800 °C. A 100 h continuous operation of this process was carried out and the result indicates the feasibility for practical applications.

**KEY WORDS:** dehydrogenation; oxygen separation; membrane reactor; ethane; ethylene.

## 1. Introduction

In the petrochemical industry, more than 60% of products obtained by catalytic processes, including some huge commercial processes such as oxidation of *n*-butane to maleic anhydride, are produced *via* oxidation [1,2]. The difficulties in this process lie in the fact that intermediates and target products, *i.e.*, olefin and oxygenates, are usually more reactive than the raw materials; alkanes, therefore, are easily deeply oxidized to  $CO_x$ . As a result, the selectivity for the target products is significantly lowered. Alternatively, peroxides, such as hydrogen peroxide [3], alkyl hydroperoxides or iodosylbenzene [4], are used as oxidants to control the deep oxidation of products. However, these peroxides are expensive and their production is harmful to the environment. Therefore, the most attractive oxidant for the chemical industry is molecular oxygen,  $O_2$ , because of its low cost and less environmental contamination. The crucial step in using  $O_2$  as an oxidant is to prevent the products from being deeply oxidized by this oxidant. Several experiments were reported up to date on protecting reactants from being attacked directly by  $O_2$ . One reduced the contact time between  $O_2$  and reactants to less than  $10^{-3}$  second in order to prevent further oxidation of the products [5–7]. The other employed a regioselective catalyst to terminally oxidize the linear alkanes by  $O_2$  [8]. A successful industrial processing example is the use of a metal oxide as an oxygen transfer agent in a periodic shift reactor, which has been used in the ammoxidation of propylene to acrylonitrile [9] and of metaxylene to

isophthalonitrile [10]. In these reactions, the metal oxide participates in a series of redox steps. This reaction strategy results in a higher selectivity in comparison with the conventional method in which hydrocarbon and oxygen are simultaneously in contact with an oxidation catalyst. However, these processes can only be operated periodically, and a catalyst that is physically and chemically more stable is to be developed to sustain repeated reduction-oxidation cycles [11].

We report the results of the oxidative dehydrogenation of ethane to produce ethylene using an oxygen permeable mixed ion and electron conducting membrane (OPMIECM) [12–22]. The mechanism of our reaction process is shown in figure 1. Molecular  $O_2$  (in air) at the air side of the OPMIECM obtain electrons from the surface of the OPMIECM to form  $O^{2-}$  species (lattice oxygen). Sequentially, the lattice oxygen is transported through the OPMIECM to the reaction side. Once the reaction side is reached, lattice oxygen will react quickly with ethane on the surface of the OPMIECM before it recombines to molecular oxygen. Local charge neutrality is maintained by the joint diffusion of oxygen vacancies and electrons. Since lattice oxygen converted from  $O_2$  by the OPMIECM is continuously supplied to the reaction system, the selectivity of the oxidation reaction can be controlled at a very high level.

## 2. Experiments

Our OPMIECM reactor is illustrated schematically in figure 2. The material of the OPMIECM is  $Ba_{0.5}Sr_{0.5}Co_{0.8}Fe_{0.2}O_{3-\delta}$  recently developed in our laboratory. A more detailed synthesis process can be

\* To whom correspondence should be addressed.  
E-mail: vangws@ms.dicp.ac.cn

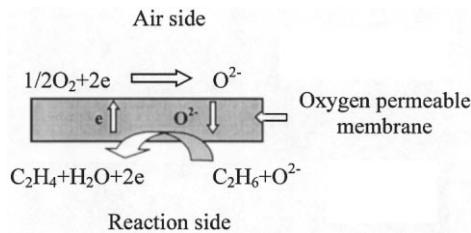


Figure 1. Schematic representation of oxidative dehydrogenation of ethane to ethylene in the OPMIECM reactor.

found in our previous papers [23,24]. The permeation area of the OPMIECM disk is  $0.813\text{ cm}^2$ . 10%  $\text{C}_2\text{H}_6$  + 90% He was fed to the reaction side, while air was fed to the air side. The inlet gas flow rates were controlled with mass flow controllers (models D07-7A/ZM). Both reaction side and air side of the reactor were maintained at atmospheric pressure. The online gas chromatograph (HP6890) was equipped with two automatic valves, a sample valve and a bypass valve, and the HP Chemstation computer software for data collection and analysis. A serial/bypass configuration was arranged for two isothermal columns ( $80^\circ\text{C}$ ), Porapak Q and molecular sieve 13X. The injection of sample gases directed the mixture of  $\text{H}_2$ ,  $\text{O}_2$ ,  $\text{N}_2$ ,  $\text{CH}_4$ ,  $\text{CO}$ ,  $\text{CO}_2$ ,  $\text{C}_2\text{H}_4$  and  $\text{C}_2\text{H}_6$  through the Porapak Q.  $\text{H}_2$ ,  $\text{O}_2$ ,  $\text{N}_2$  and  $\text{CO}$  were eluted earlier than  $\text{CH}_4$ ,  $\text{CO}_2$ ,  $\text{C}_2\text{H}_4$  and  $\text{C}_2\text{H}_6$  from the Porapak Q column and then quickly entered the serial-arranged molecular sieve 13X column. Before the  $\text{H}_2$ ,  $\text{O}_2$ ,  $\text{N}_2$  and  $\text{CO}$  were eluted from the molecular sieve 13X column, a bypass valve was activated to deaden the 13X column and direct the outlet of the Porapak Q column to the thermal conductivity detector. Once  $\text{CH}_4$ ,  $\text{CO}_2$ ,  $\text{C}_2\text{H}_4$  and  $\text{C}_2\text{H}_6$  had eluted from the Porapak Q, the valve was again activated, and the  $\text{H}_2$ ,  $\text{O}_2$ ,  $\text{N}_2$  and  $\text{CO}$  were eluted from the molecular sieve column 13X to the detector. An external standardization was used for product analysis. Multiple-point calibration curves were created and recalibrated routinely for long-term studies. The quantity of  $\text{H}_2\text{O}$  was calculated by hydrogen atomic balance. The oxygen permeation rate

was calculated from the measured outlet flow rate and the mole fractions of oxygen-containing product gases, such as  $\text{CO}$ ,  $\text{CO}_2$ ,  $\text{O}_2$  and  $\text{H}_2\text{O}$ . The carbon balance during all of the experiments was within 5%. The separation of  $\text{O}_2$  and  $\text{N}_2$  was crucial for leak checking on the membrane tube and the sealing. The leakage of oxygen could be calculated from the leakage of nitrogen. In the reaction experimental results, the leakage of oxygen, which accounted for 0 to 2% of the total oxygen flux, was subtracted from the total oxygen flux.

### 3. Results and discussion

The intrinsic catalytic behavior of the OPMIECM reactor based on BSCFO for oxidative dehydrogenation of ethane to ethylene was performed in the reactor, as shown in figure 2. After sealing at high temperature ( $1040^\circ\text{C}$ ), the furnace was cooled down to the temperatures of interest, then air was introduced to the air side and the feed (10%  $\text{C}_2\text{H}_6$  + 90% He) was introduced to the reaction side. In all the experiments, air flow rate was 300 ml/min. The species detected in the eluted gas of the reaction side were  $\text{C}_2\text{H}_4$ ,  $\text{C}_2\text{H}_6$ ,  $\text{H}_2\text{O}$ ,  $\text{CO}_2$ ,  $\text{CO}$  and  $\text{CH}_4$ . There was no  $\text{O}_2$  detected in the eluted gas, which indicated that  $\text{O}_2$  was consumed completely in this reaction. Figure 3 shows the temperature effect on the performance of oxidative dehydrogenation of ethane to ethylene in the OPMIECM reactor when the feed flow rate was kept constant at 30 ml/min. As shown in figure 3, with the increase of reaction temperature from  $700^\circ\text{C}$  to  $850^\circ\text{C}$ , the  $\text{C}_2\text{H}_6$  conversion increased from 18.0% to 96.5%, the  $\text{C}_2\text{H}_4$  selectivity decreased from 91.0% to 60.2%, and the yield of  $\text{C}_2\text{H}_4$  reached the maximum value (67.4%) at  $800^\circ\text{C}$ , then decreased slightly between  $800^\circ\text{C}$  and  $900^\circ\text{C}$ . The oxygen permeation of the membrane increased with the increase of temperature, and the oxygen permeation flux in Air/ $\text{C}_2\text{H}_6$ -He gradient ( $J_{\text{O}_2} = 1.72\text{ ml/cm}^2\text{ min}$ , at  $800^\circ\text{C}$ ) is about two times that in Air/He gradient ( $J_{\text{O}_2} = 1.0\text{ ml/cm}^2\text{ min}$ , at  $800^\circ\text{C}$ ). However, when we

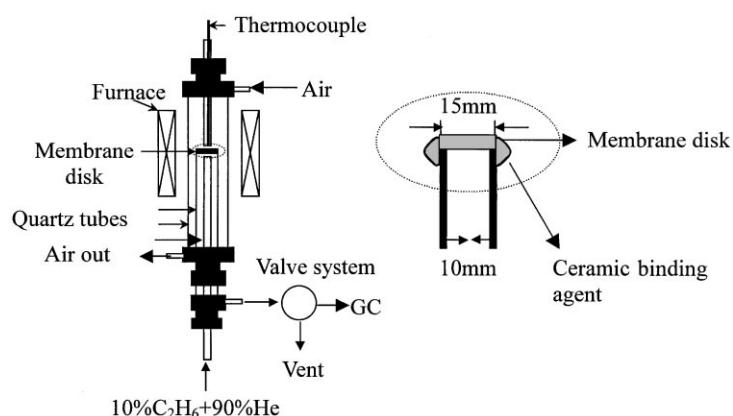


Figure 2. Schematic diagram of the OPMIECM reactor for ethane oxidative dehydrogenation to ethylene.

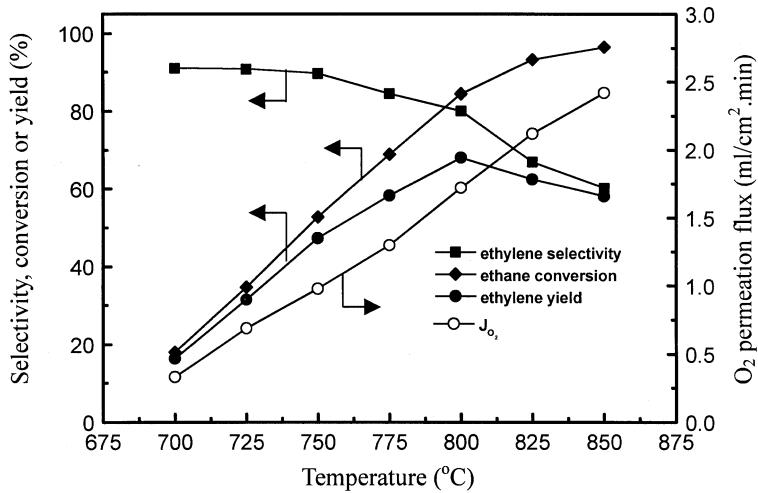


Figure 3. Effect of temperature on the performance of oxidative dehydrogenation of ethane and oxygen permeation flux.

use gaseous O<sub>2</sub> transport through the membrane to partially oxidize ethane to syngas, the oxygen permeation flux will be about eight times higher than that in Air/He gradient [25]. These results indicated that the reactivity of lattice oxygen (O<sup>2-</sup>) is much lower than that of gaseous O<sub>2</sub>, so that the deep oxidation of ethane and/or ethylene was suppressed, and the selectivity of ethylene was high. Since the yield of ethylene was the highest at a temperature of 800 °C, 800 °C was selected as a standard temperature for further experiments.

Figure 4 shows the effect of the feed flow rates on the performance of oxidative dehydrogenation of ethane to ethylene in the OPMIECM reactor. It can be seen that with the increase of the feed flow rate, the ethylene selectivity increased, but the ethane conversion decreased. The lower ethylene selectivity at lower feed flow rate was due to the fact that a longer residence time often means a higher probability of oxidation of the valuable intermediate produced. The ethylene yield was reached at the highest value when the feed flow rate was 30 ml/min. Based on the oxygen balance, the amount of permeated

oxygen at different feed flow rates can be calculated, and the result is shown in figure 5. As indicated in figure 5, with the increase of the flow rate of feed from 10.63 ml/min to 49.73 ml/min, the permeated oxygen of the OPMIECM increased from 1.26 ml/cm<sup>2</sup> min to 2.19 ml/cm<sup>2</sup> min, but the mole ratio of oxygen to ethane decreased from 0.92 to 0.3. When the feed flow rate was 30 ml/min, the mole ratio of oxygen to ethane was 0.46, which is close to the stoichiometric ratio for the selective oxidation of ethane by O<sub>2</sub> to produce ethylene. Therefore, the ethylene yield was the highest when the feed flow rate was 30 ml/min in our experiment.

As indicated in our mechanism of reaction in the OPMIECM reactor, we attributed the high selectivity to ethylene to reaction between ethane and lattice oxygen. To verify this speculation, we designed a periodic shift reactor using OPMIECM oxides (containing O<sup>2-</sup> intrinsically) as a catalyst, as shown in figure 6(b). In this experiment, the feed flow rate was controlled at 30 ml/min and reaction temperature was kept at 800 °C. O<sub>2</sub> and ethane diluted with helium were fed to the reactor alternately. When O<sub>2</sub> was fed to the reaction side, the lattice oxygen (O<sup>2-</sup>) could be formed in membrane oxide by the reactions O<sub>2</sub>(g)  $\leftrightarrow$  O<sub>2</sub>(ad)  $\leftrightarrow$  2O<sup>2-</sup>(s). In order to sweep out the gaseous oxygen (O<sub>2</sub>(g)) and adsorbed oxygen (O<sub>2</sub>(ad)) on the OPMIECM oxides, the reactor was purged with helium before the ethane was introduced into the line. When ethane diluted with helium was supplied to the reactor, ethane directly reacted with the lattice oxygen (O<sup>2-</sup>) of the OPMIECM oxides. Since the reaction between ethane and O<sup>2-</sup> was transient in this reactor, the measurements were made before O<sup>2-</sup> was completely consumed. The result in this reactor was very similar to that in the OPMIECM, as shown in table 1. The similarity in the results between these two reactors suggests that our mechanism of reaction in the OPMIECM is correct.

In order to elucidate the role of gas-phase O<sub>2</sub> in the deep oxidation of ethylene to CO<sub>x</sub>, we also carried out

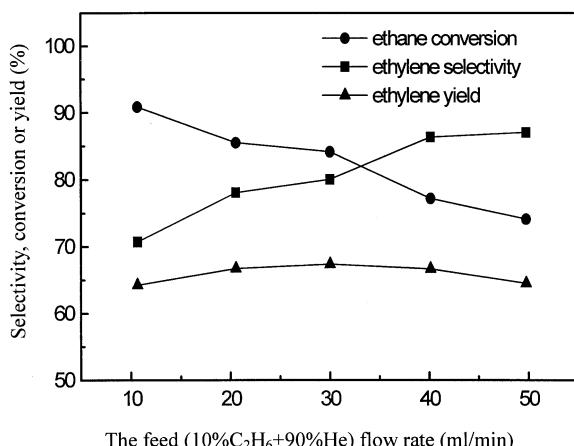


Figure 4. Effect of feed flow rates on the performance of oxidative dehydrogenation of ethane in the OPMIECM reactor at 800 °C.

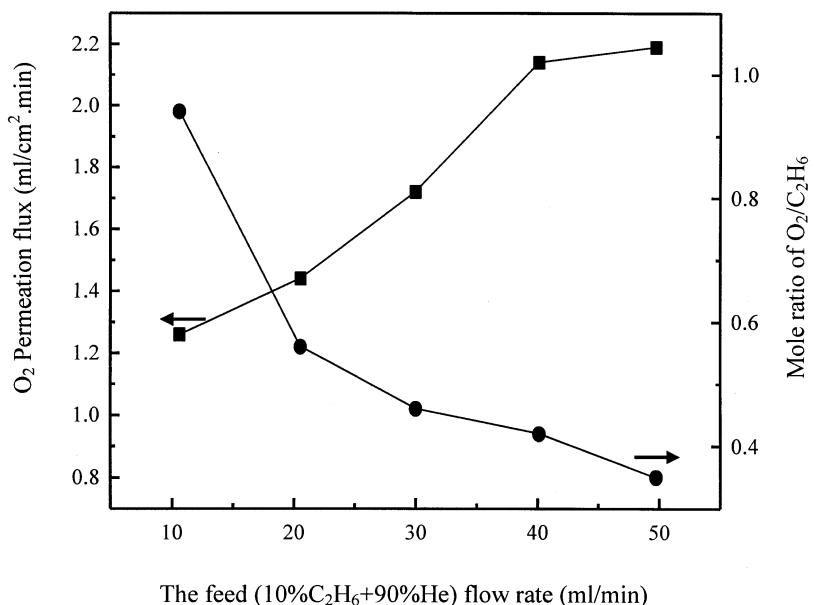


Figure 5. Effect of feed flow rate on the permeated oxygen of the OPMIECM and the mole ratio of O<sub>2</sub>/C<sub>2</sub>H<sub>6</sub> in the OPMIECM reactor at 800 °C.

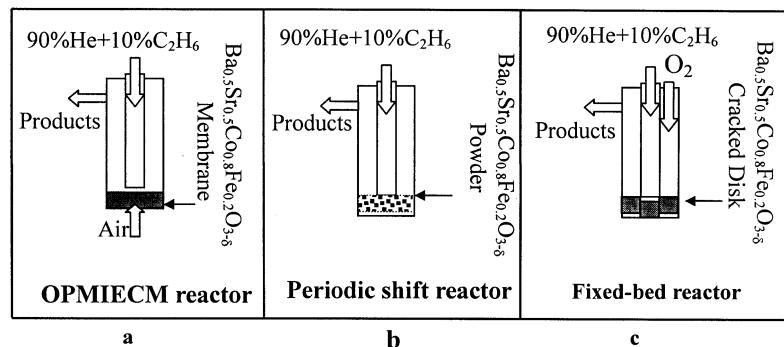


Figure 6 (a-c). Comparative study of oxidative dehydrogenation of ethane to ethylene in different reactors at 800 °C.

the reaction of the oxidative dehydrogenation of ethane in a conventional fixed-bed reactor with a catalyst of broken OPMIECM fed with pure O<sub>2</sub>, as shown in figure 6(c). It is important to note that the size and shape of the three reactor types are the same. To eliminate the non-catalytic homogeneous reaction in the gas phase, we introduced ethane and O<sub>2</sub> to the reaction system separately before they reach the surface of the catalyst. In this experiment, 30 ml/min 10% ethane + 90% He, at a reaction temperature of 800 °C, was fed through the inner tube and 1.4 ml/min O<sub>2</sub> equal to the

oxygen permeation flux of the membrane was fed through the outer tube. The result is listed in table 1. It shows that only 53.7% selectivity to ethylene and more than 36% CO<sub>x</sub> were obtained in this reactor, indicating that molecular oxygen is responsible for the deep oxidation of ethylene to CO<sub>x</sub>. That the ethylene selectivity in the OPMIECM reactor is similar to that in the periodic shift reactor and much higher than that in the fixed-bed reactor indicates that the OPMIECM can provide lattice oxygen rather than gaseous oxygen for oxidative dehydrogenation of ethane to ethylene. This mechanism

Table 1  
Typical results of oxidative dehydrogenation of ethane to ethylene in different reactors at 800 °C.

Reactor types	C <sub>2</sub> H <sub>6</sub> conversion (%)	Product selectivity (%)			
		C <sub>2</sub> H <sub>4</sub>	CH <sub>4</sub>	CO	CO <sub>2</sub>
OPMIECM reactor	84.17	80.06	5.74	6.43	7.87
Periodic shift reactor	85.61	88.22	4.56	7.22	0
Fixed-bed reactor	83.63	53.71	9.5	13.92	22.85

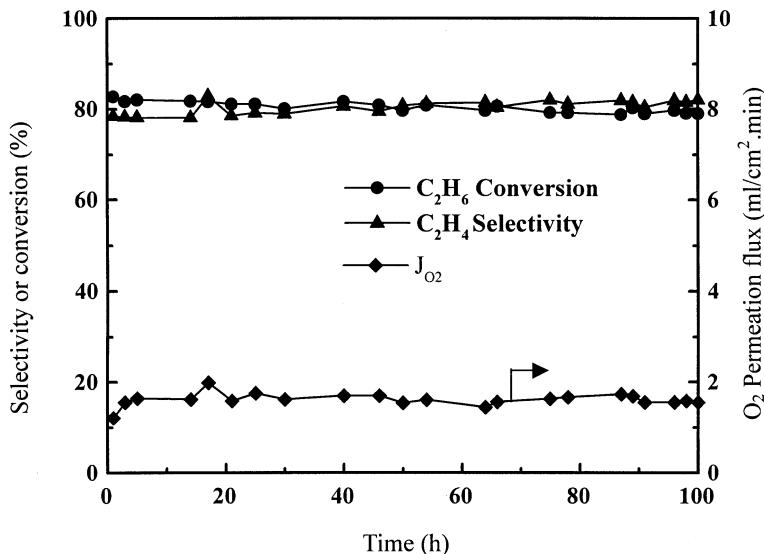


Figure 7. Long-term operation of the OPMIECM reactor for oxidative dehydrogenation of ethane to ethylene at 800 °C.

is also proven in our previous paper [26]. From table 1, we can also see that the ethylene selectivity in the OPMIECM reactor is slightly lower than that in the periodic shift reactor. The reason is that a little part of the lattice oxygen recombined to gaseous oxygen, which reacted with ethylene to form  $\text{CO}_x$ .

We carried out a 100 h experiment of the oxidative dehydrogenation of ethane to ethylene in the OPMIECM reactor to test the long-term operation capability of this reactor for practical applications. The feed flow rate was 30 ml/min and the reaction temperature was 800 °C. The result is shown in figure 7. In this experiment, the ethylene selectivity, the ethane conversion and the oxygen flux at reaction conditions were maintained at ~80%, ~82% and ~1.6 ml/ $\text{cm}^2\text{ min}$  respectively. This result indicates that  $\text{O}^{2-}$  species can be continuously supplied by the OPMIECM, and the reaction process can be continuously operated in the OPMIECM reactor with high ethylene selectivity and ethane conversion.

#### 4. Conclusions

Based on our results, it is concluded that the selectivity to ethylene resulting from the selective oxidation of ethane can be greatly improved in an OPMIECM reactor. This process has several additional advantages over the conventional oxidative dehydrogenation process: (1) Oxygen can be obtained directly from air *via* membrane separation instead of extracted from cryogenic distillation. (2) The reaction zone is free of gaseous  $\text{O}_2$ , so that the operation can be controlled smoothly without the danger of explosion. It is possible to apply this novel approach for a wider range of selective oxidation reactions with the exploration of new catalytic membrane materials.

#### Acknowledgments

The authors gratefully acknowledge financial support from the Ministry of Science and Technology, China (Grant No. G1999022401) and the National Advanced Materials Committee of China (Grant No. 715-006-0122).

#### References

- [1] J. Haber, Stud. Surf. Sci. Catal. 72 (1992) 279.
- [2] S. Albonetti, F. Cavani and F. Trifiro, Catalysis Reviews, Science & Engineering 38(4) (1996) 413.
- [3] T. Tatsumi, M. Nakamura, S. Negishi and H. Tominaga, J. Chem. Soc. Chem. Commun. (1990) 476.
- [4] J.A. Smegal and C.L. Hill, J. Am. Chem. Soc. 105 (1983) 3515.
- [5] D.A. Hickman and L.D. Schmidt, Science 259 (1993) 343.
- [6] D.A. Goetsch and L.D. Schmidt, Science 271 (1996) 1560.
- [7] A.S. Bodke, D.A. Olschki, L.D. Schmidt and E. Ranzi, Science 285 (1999) 712.
- [8] J.M. Thomas, R. Raja, G. Sankar and R.G. Bell, Nature 398 (1999) 227.
- [9] J.L. Callahan, R.K. Grasselli, E.C. Milberger and H.A. Stecker, I&EC Product Res. & Dev. 9 (1970) 134.
- [10] M.N. Schevendeman, R. McBride, D. Reuter and M. Isaacs, Chemical Processing, July (1983) 100.
- [11] E.A. Mamedov and V.C. Corberan, Appl. Catal. A 127 (1995) 1.
- [12] B.C.H. Steele, Current Opinion in Solid State & Materials Science 1 (1996) 684.
- [13] P.J. Gellings and H.J.M. Bouwmeester, Catal. Today. 58(1) (2000) 1.
- [14] V.V. Kharton, E.N. Naumovich and A.V. Nikolaev, J. Membr. Sci. 111 (1996) 149.
- [15] T.M. Gur, A. Belmer and R. Ahuggins, J. Membr. Sci. 75 (1992) 151.
- [16] L. Qiu, T.H. Lee, L.M. Liu, Y.L. Yang and A.J. Jacobson, Solid State Ionics 76 (1995).
- [17] Y. Teraoka, T. Nobunaga, K. Okamoto, N. Miura and N. Yamazoe, Solid State Ionics 48 (1991) 207.
- [18] C.Y. Tsai, A.G. Dixon, W.R. Moser and Y.H. Ma, AIChE J. 43 (1997) 2741.

- [19] U. Balachandran, J.T. Dusek, R.L. Mieville, R.B. Poeppel, M.S. Kleefish, S. Pei, T.P. Kobylnski, J. Faber and C.A. Bose, *Appl. Catal. A* 133 (1995) 219.
- [20] J.E. Elshof, H.J.M. Bouwmeester and H. Verweij, *Appl. Catal. A* 130 (1995) 195.
- [21] S. Xu and W.J. Thomson, *AIChE J.* 43 (1997) 2731.
- [22] Y. Zeng, Y.S. Lin and S.L. Swartz, *J. Membr. Sci.* 150 (1998) 87.
- [23] Z.P. Shao, W.S. Yang, Y. Cong, H. Dong, J.H. Tong and G.X. Xiong, *J. Membr. Sci.* 172 (2000) 177.
- [24] H. Dong, Z.P. Shao, G.X. Xiong, J.H. Tong, S.S. Sheng and W.S. Yang, *Catal. Today* 67 (2001) 3.
- [25] H.H. Wang, Y. Cong and W.S. Yang, *J. Membr. Sci.* in press.
- [26] H.H. Wang, Y. Cong and W.S. Yang, *Chem. Comm.* 14 (2002) 1468.